

Long-distance entanglement of purification in conformal field theory

Hugo A. Camargo,^{1,2,*} Lucas Hackl,^{3,†} Michal P. Heller,^{1,‡} Alexander Jahn,^{2,§} and Bennet Windt^{4,¶}

¹Max-Planck-Institut für Gravitationsphysik, Am Mühlenberg 1, 14476 Potsdam-Golm, Germany

²Dahlem Center for Complex Quantum Systems,

Freie Universität Berlin, Arnimallee 14, 14195 Berlin, Germany

³School of Mathematics and Statistics & School of Physics,

The University of Melbourne, Parkville, VIC 3010, Australia

⁴Blackett Laboratory, Imperial College London, Prince Consort Road, SW7 2AZ, UK

Quantifying entanglement properties of mixed states in quantum field theory via entanglement of purification is a new and challenging subject. In this work, we study entanglement of purification for two intervals far away from each other in the vacuum of a conformal field theory on a lattice. Our main finding is that the decay of the entanglement of purification is enhanced with respect to the one for the mutual information by a logarithm of the distance between the intervals. We explicitly derive this behaviour in the critical Ising spin chain as well as for free fermions. Furthermore, we corroborate it with a general argument valid for any conformal field theory with a gapped spectrum of operators arising as a continuum description of a lattice model.

Introduction. Understanding quantum information properties of quantum field theories (QFTs) and, through holography [1–3], also of gravity has been an important line of research of the past two decades [4–8]. The object of primary interest has been entanglement entropy (EE) of spatial subregions in QFT. To this end, starting from a globally pure state (here the vacuum $|0\rangle$) and a spatial subregion A and its complement \bar{A} , one defines a reduced density matrix in A

$$\rho_A = \text{tr}_{\bar{A}} |0\rangle \langle 0|. \quad (1)$$

EE is then defined as its von Neumann entropy

$$S_A = S(\rho_A) \equiv -\text{tr}_A \rho_A \log \rho_A. \quad (2)$$

EE is an ultraviolet-divergent quantity due to correlations at arbitrarily short distances in QFT and its computation requires introducing a regulator. This can be done using Gaussian techniques [9–13] for interesting states in free QFTs, whereas closed form results and tractable limits in two-dimensional CFTs follow from framing it as an analytic continuation of correlation functions of primary operators [14–19], while in two spacetime dimensions, one can also employ tensor network techniques to efficiently compute EE [20, 21]. In strongly-coupled holographic QFTs, computing it reduces to a geometric problem of finding minimal surfaces [22–25]. As a quantum-theoretic quantity, it is a reliable measure of entanglement between A and \bar{A} in globally pure states.

In the present work, we will be concerned with conformal field theories (CFTs) emerging as a long-distance limit of lattice models and the ultraviolet cut off will be provided by an underlying lattice with spacing δ . At the same time, we will be interested in a situation in which one considers a reduced density matrix for a subsystem consisting of two parts A and B . One quantity to consider in this case is the *mutual information* (MI) defined in terms of EE as

$$I(A : B) = S_A + S_B - S_{AB}. \quad (3)$$

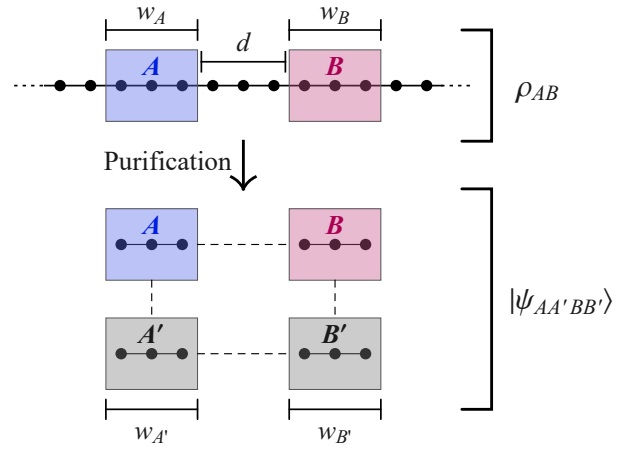


FIG. 1. Entanglement of purification on an infinite lattice: The mixed state ρ_{AB} on a subsystem of two disjoint regions AB separated by $N_d \equiv \frac{d}{\delta}$ sites is purified to a state with auxiliary factors A' and B' , taken to be of the same size $N_A \equiv w_A/\delta$ and $N_B \equiv w_B/\delta$ as A and B , respectively, where δ is the lattice spacing. Here we mostly consider $N_A = N_B$.

Another quantity of significant recent interest in such a setup is the *entanglement of purification* (EoP) [26], which can be regarded as a generalization of EE for bipartite mixed states. It requires purifying the reduced density matrix ρ_{AB} to a pure state $|\Psi\rangle$ in an enlarged Hilbert space consisting now of A and B supplemented by auxiliary factors A' and B' , such that $\rho_{AB} = \text{tr}_{A'B'} |\Psi\rangle \langle \Psi|$ (visualized in Fig. 1). The EoP is then defined as

$$E_P(\rho_{AB}) = \min_{\Psi} [S_{AA'}]. \quad (4)$$

EoP is intrinsically based on an optimization procedure over purifications and is by default challenging to consider in QFT. Derived from this is the distinguishing feature of EoP with respect to other correlation measures such as EE, namely that it additionally provides a particular purification of the mixed state for which the

von Neumann entropy (2) is minimum. To date, its understanding in the intersection of quantum information science and high-energy physics is based on Gaussian calculations [27–29], usage of CFT techniques with a limited range of applicability [30–32] and, finally, on a conjectured realization in holography [33, 34]. It is worth pointing out that in the latter case, EoP is conjectured to be dual to the entanglement wedge cross section [35–38] for which a variety of results have been found ranging from connections with multipartite states to thermal states (see *e.g.*, [39–49]) and is thus pivotal to the efforts of understanding bulk reconstruction in holography [50].

The aim of this letter is to to elucidate what perhaps is the simplest setting in which EoP behaves universally across CFTs and does not rely on Gaussianity nor on local conformal transformations. We achieve this by using spin chains and, more generally, lattice models in a mixture of analytic and numerical techniques.

Setup. In our analysis, we will be concerned with two-dimensional CFT and we will assume existing lattice approximation. The setting of interest to us will be two intervals of the same length w separated by a distance d , see Fig. 1. At large distances $\frac{d}{w} \gg 1$, the decay of MI (3) in CFTs takes the form

$$I(A : B) = \mathcal{N} \frac{\Gamma(\frac{3}{2})\Gamma(2\Delta + 1)}{2^{4\Delta+1}\Gamma(2\Delta + \frac{3}{2})} \times \epsilon_\Delta^2 + \dots, \quad (5)$$

where

$$\epsilon_\Delta \equiv \left(\frac{w}{d}\right)^{2\Delta} \quad (6)$$

and Δ corresponds of the scaling dimension of the lowest non-trivial operator(s) in the theory [18, 19], \mathcal{N} stands for possible degeneracy of such operators and the ellipsis denotes faster decaying terms [19, 51, 52]. This formula assumes a gap in the spectrum of scaling dimensions and we will carry over this assumption in our studies of EoP.

We will be primarily interested in the Ising model realization of the $c = \frac{1}{2}$ CFT on an infinite line, which can be described by the critical lattice Hamiltonian

$$\hat{H} \sim - \sum_{i=-\infty}^{\infty} (2\hat{S}_i^x \hat{S}_{i+1}^x + \hat{S}_i^z), \quad (7)$$

more general forms of which we discuss in the appendix. The $\hat{S}_i^{x,z}$ are spin operators defined by the Pauli matrices $\hat{S}_i^{x,z} = \frac{1}{2}\sigma_i^{x,z}$. In the Ising CFT there is a non-degenerate (*i.e.*, $\mathcal{N} = 1$ in (5)) lightest operator of a scaling dimension $\Delta = \frac{1}{8}$, often denoted as the spin field σ and corresponding to a \hat{S}_i^x lattice operator.

While it is well known that the Ising model can be mapped to a free fermion theory, the setup of interest – reduced density matrices in two disjoint intervals – is genuinely non-Gaussian [29, 53–56], as are almost all CFTs,

and we will provide more comments on this issue later in the letter.

Large-distance analytics. We start our studies by considering a subsystem AB consisting of two single sites ($w = \delta$) separated by d/δ sites in the ground state of the critical Ising model (7). The central idea is to use it as a point of departure for analytic treatment of EoP in the Ising CFT and as a guidance for a generic situation.

While the reduced density matrix ρ_{AB} is non-Gaussian, following [55] one can still use Gaussian techniques to deduce its asymptotic behaviour as $\frac{d}{w} \rightarrow \infty$ (or, equivalently, $\epsilon_{\frac{1}{8}} \rightarrow 0$). This leads to

$$\rho_{AB} \sim \begin{pmatrix} D & 0 & 0 & C\epsilon_{\frac{1}{8}} \\ 0 & E & C\epsilon_{\frac{1}{8}} & 0 \\ 0 & C\epsilon_{\frac{1}{8}} & E & 0 \\ C\epsilon_{\frac{1}{8}} & 0 & 0 & F \end{pmatrix} \quad (8)$$

with $D = \frac{1}{4} + \frac{1}{\pi} + \frac{1}{\pi^2}$, $E = \frac{1}{4} - \frac{1}{\pi^2}$, $F = \frac{1}{4} - \frac{1}{\pi} + \frac{1}{\pi^2}$, $C = \frac{\exp(3\zeta'(-1))}{2^{23/12}}$ and a possible contribution of the order $\epsilon_{\frac{1}{8}}^2$ vanishes, see appendix for a derivation. We represent ρ_{AB} in the basis $|\uparrow\uparrow\rangle, |\uparrow\downarrow\rangle, |\downarrow\uparrow\rangle$ and $|\downarrow\downarrow\rangle$ with the factor ordering AB . The anti-diagonal terms $C\epsilon_{\frac{1}{8}}$ encode long distance correlations between \hat{S}_i^x at the two sites.

The continuum limit corresponding to the Ising CFT is obtained by keeping d/w (or, equivalently, $\epsilon_{\frac{1}{8}}$) fixed and taking δ/w to 0. We will see that considering only a few lattice sites is sufficient to describe the qualitative and approximate quantitative behaviour of the continuum limit. To demonstrate this, we use (8) to calculate the large distance asymptotics of the MI (3) and compare it with (5). The EE of the disjoint system follows from the eigenvalue spectrum of (8). Its four eigenvalues μ_j are

$$\mu_{1,2} = \frac{1}{4} - \frac{1}{\pi} \pm C\epsilon_{\frac{1}{8}}, \quad (9a)$$

$$\mu_{3,4} = \frac{1}{4} + \frac{1}{\pi} \pm \sqrt{\frac{1}{\pi^2} + C^2\epsilon_{\frac{1}{8}}^2}, \quad (9b)$$

from which we can directly compute the EE for AB

$$S = - \sum_j \mu_j \log \mu_j. \quad (10)$$

Note that in the following we will denote eigenvalues of any density matrix by μ_j .

This analysis leads to the Ising model prediction for a spin MI at large separations of the following form

$$I(A : B) \sim \left(\frac{4\pi^2}{\pi^2 - 4} + \frac{\pi}{2} \log \frac{4 + 4\pi + \pi^2}{4 - 4\pi + \pi^2} \right) C^2 \times \epsilon_{\frac{1}{8}}^2. \quad (11)$$

Comparing this formula with the CFT analytics (5) for $\Delta = \frac{1}{8}$, we see an exact match in the power-law behaviour. Furthermore, the prefactor in (11) evaluates to

approximately 0.2978, which is only 3.6% off from the continuum value of about 0.309 predicted by (5).

Furthermore, explicit *numerical* calculations using the full reduced density matrix ρ_{AB} show that the continuum value of the prefactor is well attained at large distances already for $w = 2\delta$ and 3δ , see Fig. 2(a). This provides a strong support to consider (8) as a good starting point for an analysis of long distance behaviour of EoP in the Ising CFT.

EoP of minimal subsystems. In the limit of an infinite distance between the two single site subsystems, we purify (8) by the state $|\psi^{(0)}\rangle$ with Schmidt decomposition

$$|\psi^{(0)}\rangle = \sqrt{D} |\downarrow\downarrow\downarrow\downarrow\rangle + \sqrt{E} (|\uparrow\downarrow\uparrow\downarrow\rangle + |\downarrow\uparrow\downarrow\uparrow\rangle) + \sqrt{F} |\uparrow\uparrow\uparrow\uparrow\rangle, \quad (12)$$

where the convention for factors ordering in the purification is $ABA'B'$. Note that in this analysis we assume that a minimal purification from two to four spin degrees of freedom suffices and we will subsequently provide supporting numerical evidence and an additional discussion.

Moving on, we *supplement* this purification with finite distance corrections up to second order in $\epsilon_{\frac{1}{8}}$ as

$$|\psi\rangle \sim |\psi^{(0)}\rangle + \epsilon_{\frac{1}{8}} |\psi^{(1)}\rangle + \frac{1}{2}\epsilon_{\frac{1}{8}}^2 |\psi^{(2)}\rangle. \quad (13)$$

We will optimize over $|\psi^{(1)}\rangle$ and $|\psi^{(2)}\rangle$ subject to the normalization constraint $\langle\psi|\psi\rangle = 1$ order by order in $\epsilon_{\frac{1}{8}}$.

We further require $\rho_{AB}^{(1)} = |\psi^{(0)}\rangle\langle\psi^{(1)}| + |\psi^{(1)}\rangle\langle\psi^{(0)}|$ and $\rho_{AB}^{(2)} = |\psi^{(0)}\rangle\langle\psi^{(2)}| + |\psi^{(2)}\rangle\langle\psi^{(0)}| + 2|\psi^{(1)}\rangle\langle\psi^{(1)}|$ to satisfy

$$\rho_{AB}^{(1)} = \begin{pmatrix} & & C \\ & C & \\ C & & \end{pmatrix} \quad \text{and} \quad \rho_{AB}^{(2)} = 0, \quad (14)$$

which follows from (8). Combining the normalization condition for $|\psi\rangle$ with constraints (14) allows to systematically eliminate free parameters in $|\psi^{(1)}\rangle$ and $|\psi^{(2)}\rangle$. In order to compute $S_{AA'}$, which is the building block of EoP (4), we need to find the four eigenvalues μ_j of

$$\rho_{AA'} = \rho_{AA'}^{(0)} + \epsilon_{\frac{1}{8}} \rho_{AA'}^{(1)} + \frac{1}{2}\epsilon_{\frac{1}{8}}^2 \rho_{AA'}^{(2)}. \quad (15)$$

We expect the pattern

$$\mu_0 \sim 1 - \alpha_{\text{tot}} \epsilon_{\frac{1}{8}}^2 \quad \text{and} \quad \mu_{j>0} \sim \alpha_j \epsilon_{\frac{1}{8}}^2, \quad (16)$$

where $\alpha_{\text{tot}} = \sum_{j>0} \alpha_j$ and here $j > 0$ runs from 1 to 3. Computing the individual α_j requires extensive work, but α_{tot} can be deduced by expanding

$$\text{Tr}(\rho_{AA'}^2) = \sum_j \mu_j^2 \sim 1 - 2\alpha_{\text{tot}} \epsilon_{\frac{1}{8}}^2. \quad (17)$$

Its RHS leads to the explicit formula

$$\begin{aligned} \frac{\alpha_{\text{tot}}}{C^2} &= \frac{(\pi-2)x_2^2 - 2\sqrt{\pi^2-4}x_{12}x_2 - 2\sqrt{\pi^2-4}x_3x_8}{2+\pi} \\ &+ \frac{\pi((\pi-2)\pi-4)x_3^2 + 8(x_3^2 + \pi^3)}{(\pi-2)(2+\pi)^2} - \frac{4\pi\sqrt{\pi^2-4}x_7}{\pi^2-4} \\ &+ \frac{2(4+\pi^2)x_4^2 - 4(\pi-2)\pi x_4}{(2+\pi)^2} + 2x_7^2 + (x_8^2 + x_{12}^2), \end{aligned} \quad (18)$$

where x_i are remaining parameters in $|\psi^{(1)}\rangle = \sum_i x_i |\phi_i\rangle$, where $|\phi_i\rangle$ is the basis of $\mathcal{H}_{ABA'B'}$ ordered as in (12). The expansion of the unoptimized EE (10), which underlies the definition of EoP (4), takes the form

$$S_{AA'} = \alpha_{\text{tot}} \epsilon_{\Delta}^2 \log(\epsilon_{\Delta}^{-2}) + \left(\sum_{j>0} \alpha_j (1 - \log \alpha_j) \right) \epsilon_{\Delta}^2, \quad (19)$$

where $\Delta = \frac{1}{8}$, shown later to hold for a general Δ .

In order to find the EoP, we need to minimize over the x_i to find the smallest possible α_{tot} , which can be done *analytically* and leads to

$$\alpha_{\text{tot}} = \frac{4\pi^4 C^2}{\pi^4 - 16} \approx 0.12445. \quad (20)$$

The non-vanishing α_{tot} shows that the resulting EoP obtained from (19) has the leading order long-distance behaviour enhanced with respect to that of MI (11) by a logarithm of the distance.

This is our main finding and the remaining part of our letter is devoted to providing further support for its correctness from the point of view of the continuum limit and robustness of minimal purifications, as well as discussing its generalization in a generic CFT with a gap in the operator spectrum in a lattice representation.

When it comes to the *subleading* long-distance behaviour encapsulated by $\left(\sum_{j>0} \alpha_j (1 - \log \alpha_j) \right)$, we would need to extract the individual α_j and optimize over the remaining parameters. While it is plausible this can be also done analytically, we skip this tedious step and in the following will simply resort to numerics.

Numerical results. Our analytic derivation of the EoP is in excellent agreement with fully numerical studies. Note that the latter do not rely on the $\epsilon_{\frac{1}{8}}$ -expanded density matrix (8), but rather take full numerically evaluated ρ_{AB} as an input.

Our numerical results for minimal purifications (from 1+1 to 1+1+1+1 degrees of freedom, as in the analytic derivation, and from 2+2 to 2+2+2+2) are depicted in Fig. 2(c). We find a rapid convergence to (19) with the distance. The leading decay slope for $w = \delta$ corroborates our analytical prediction (20), with the coefficient of the subleading decay numerically predicted to be approximately 0.423. The $w = 2\delta$ data gives

$$E_P \sim 0.128 \epsilon_{\frac{1}{8}}^2 \log(\epsilon_{\frac{1}{8}}^{-2}) + 0.440 \epsilon_{\frac{1}{8}}^2 \quad (21)$$

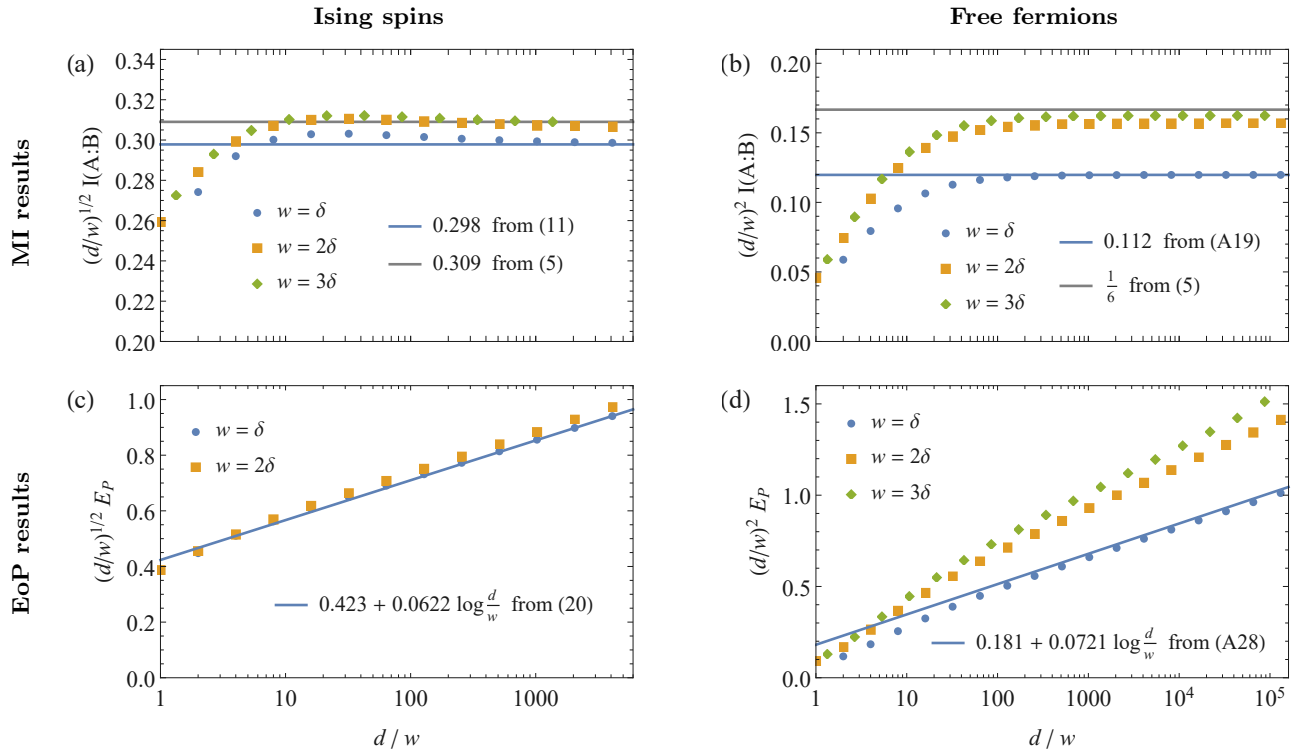


FIG. 2. Numerical data for MI and EoP for spins and fermions, rescaled by the power-law contribution $\epsilon_{\Delta}^2 = (w/d)^{4\Delta}$ of the respective dominant term with $\Delta = \frac{1}{8}$ for Ising spins and $\Delta = \frac{1}{2}$ for free fermions. The analytical predictions for $w = \delta$ are derived in the main text for the Ising spins and in the appendix for free fermions.

We see that the leading fall-off coefficient changes from the analytic prediction at $w = \delta$ in (20) by only 2.6% and the subleading fall-off coefficient by only 3.9%.

We found generating data numerically for $w = 3\delta$ challenging, since, on one hand, this requires dealing with much bigger matrices making the calculating slower (see appendix) and, on the other, requires maintaining rather high accuracy due to the need of keeping fine large distance corrections. However, taking MI as a guidance, as discussed below (11), one sees there very similar deviations between $w = \delta$ and $w = 2\delta$ and we therefore would expect very little difference between large-distance behaviour of EoP for $w = 2\delta$ and $w = 3\delta$.

Regarding corroborations, a key question concerns the dimensions of the initial and enlarged Hilbert spaces. In our setup, when purifying the state of a system with $N_A + N_B$ degrees of freedom by adding $N_{A'} + N_{B'}$ additional ones (see also Fig. (1)), there is *a priori* no constraint on $N_{A'}$, $N_{B'}$ other than the basic requirement following from the definition of the Schmidt decomposition that $N_{A'} + N_{B'} \geq N_A + N_B$. However, we show in the appendix that the choice of *minimal purifications* corresponding to $N_{A'} + N_{B'} = N_A + N_B$ and made so far yields the true minimum of EE, so long as we choose $N_{A'} = N_A$ and $N_{B'} = N_B$. This was already shown in [57] based on ideas in [58] for the EoP for Gaussian states (with

Gaussian purifications).

Towards generality. In our presentation so far, we followed the properties of the Ising model. However, our derivation of the scaling of the EoP is much more general and applies to any CFT with a gap in the operator spectrum that arises from a discrete lattice model at criticality [59].

To run the general argument, we only need to assume that the density operator ρ_{AB} of two subsystems A and B far away from each other takes the form

$$\rho_{AB}(\epsilon_{\Delta}) \sim \rho_A^{(0)} \otimes \rho_B^{(0)} + \epsilon_{\Delta} \rho_{AB}^{(1)} + \frac{1}{2} \epsilon_{\Delta}^2 \rho_{AB}^{(2)} + \dots, \quad (22)$$

where \dots denotes higher, not necessarily integer powers of ϵ_{Δ} and we do not make any assumptions about subsystem sizes. One can easily be convinced that (8) is precisely of this form. Furthermore, it is also clear that the ϵ_{Δ} term in (22) is crucial in order to reproduce the power-law scaling of the connected two-point function of the lowest lying scaling operators in the lattice description.

The fact that ρ_{AB} is a product state at $\epsilon_{\Delta} = 0$ implies that $\rho_{AA'}(\epsilon_{\Delta} = 0)$ of the optimal purification (*i.e.*, the one with minimal entropy $S_{AA'}$) is itself pure and thus has eigenvalues $(1, 0, \dots, 0)$. In full analogy to (16), one can perturbatively account for entanglement between A

and B by constructing a series expansion of the eigenvalues in ϵ_Δ .

Provided that the optimal purification $|\psi(\epsilon_\Delta)\rangle$ to the *truncated*¹ density matrix (22) is analytical at $\epsilon_\Delta = 0$, such that we have $|\psi(\epsilon_\Delta)\rangle \sim |\psi^{(0)}\rangle + \epsilon_\Delta |\psi^{(1)}\rangle$, the resulting $\rho_{AA'}(\epsilon_\Delta)$ must be a proper density matrix for sufficiently small positive *and* negative values of ϵ_Δ . Consequently, the leading contribution to the eigenvalues of $\rho_{AA'}(\epsilon_\Delta)$ that are the building blocks for the corresponding EE will behave in full analogy with (16), *i.e.*,

$$\mu_0 \sim 1 - \alpha_{\text{tot}} \epsilon_\Delta^2 \quad \text{and} \quad \mu_j \sim \alpha_j \epsilon_\Delta^2 \quad \text{as} \quad \epsilon_\Delta \rightarrow 0 \quad (23)$$

unless $\alpha_{\text{tot}} = 0$, when the next non-zero even power of ϵ_Δ should appear. As we have seen, spatially reduced density matrices in the Ising model give rise to $\alpha_{\text{tot}} > 0$ and we expect this to be the case in many if not all the other examples that exhibit a gap in the operator spectrum. Under this assumption, formula (19) still goes through, which is the reason why we wrote it for arbitrary Δ . This indicates that in *any* lattice model giving rise to a CFT with a gapped operator spectrum the EoP for far away regions decays with the same power as mutual information, but is enhanced by a logarithm of a distance.

Finally, since it is clearly interesting if α_{tot} is indeed non-zero in other models, we used the Jordan-Wigner mapping to perform analogous calculations in the Ising model in the fermionic representation. It is well known [29, 56, 60] that reduced density matrices of non-adjacent intervals change under this mapping, effectively removing the σ operator from local fermionic expectation values. Our calculations, incorporated in figure 2(d), reproduce the behaviour (19) with $\Delta = \frac{1}{2}$, corresponding to the fermion fields ψ and $\bar{\psi}$. The power-law part of the fall-off again matches with mutual information, see figure 2(b). Furthermore, we use this opportunity to test the convergence of MI and EoP with increasing subsystem size and reach the same conclusions as for the non-Gaussian spin results. Lattice effects at small w/δ are more pronounced for fermions than for spins, which is likely due to the smaller scaling dimension gap to the ε field with $\Delta = 1$, making higher-order terms relatively more pronounced.

Outlook. In this work, we studied the behaviour of EoP for two subsystems of width w at large distance d , finding a new log-polynomial decay law (24) of the form

$$E_P \sim \left(\frac{d}{w}\right)^{-4\Delta} \log\left(\frac{d}{w}\right) \quad \text{for} \quad d \gg w. \quad (24)$$

¹ We truncate the density matrix at the quadratic order in order to avoid contributions from non-integer powers of ϵ_Δ , which would obscure our assumption about analyticity of the purification in the vicinity of ϵ_Δ .

Our work opens a genuinely new avenue for studying EoP in QFT without restriction to free models. In the long term, we hope that it will serve as a guiding principle in developing a microscopic understanding of EoP in terms of the operator content of CFTs, from which universal behaviour of MI at large distances has previously been derived. An intermediate step in this endeavor would be to supplement our numerical code with large distance behaviour of two interval density matrices obtained in various lattice models using tensor networks. This might in particular allow to reconstruct the formula governing the coefficients in the large distance scaling of EoPs akin to (3).

When optimizing over purifications outside the Gaussian realm, one is inevitably led to vast parameter spaces that quickly exhaust desktop-scale computational resources. However, the entanglement between reasonably-sized subsystems both mixed and purified is not large and it should be possible to represent purifications as inhomogeneous matrix product states (MPS). Employing tensor network techniques that are already well developed for spin chains might allow for a better access to a continuum limit, as well as recover CFT behaviour at finite $\frac{d}{w}$. See also [34] for an earlier application of MPS to EoP.

Acknowledgements. We would like to thank Jens Eisert and Tadashi Takayanagi for collaborations on related subjects and Mari Carmen Bañuls, Djordje Radicevic, Sukhbinder Singh for correspondence and insightful discussions. We thank Johannes Knaute, Chris Pattison, Leo Shaposhnik, Viktor Svensson and Ignacio Reyes for helpful comments of the draft. The Gravity, Quantum Fields and Information group at the Max Planck Institute for Gravitational Physics (Albert Einstein Institute) is supported by the Alexander von Humboldt Foundation and the Federal Ministry for Education and Research through the Sofja Kovalevskaja Award. AJ is supported by the FQXi. HC is partially supported by the Konrad-Adenauer-Stiftung through their Sponsorship Program for Foreign Students and by the International Max Planck Research School for Mathematical and Physical Aspects of Gravitation, Cosmology and Quantum Field Theory.

Appendix

Review of critical Ising model. The Hamiltonian of the transverse Ising is given by

$$\hat{H} = - \sum_{k=1}^N \left(2J \hat{S}_k^x \hat{S}_{k+1}^x + h \hat{S}_k^z \right), \quad (A1)$$

with spin operators represented by Pauli matrices σ_α

with $\alpha \in (x, y, z)$ by

$$\hat{S}_k^\alpha \equiv \mathbb{1}^{\otimes(k-1)} \otimes \frac{\sigma_\alpha}{2} \otimes \mathbb{1}^{\otimes(N-k)}. \quad (\text{A2})$$

We also use the identification $\hat{S}_{N+1}^\alpha \equiv \hat{S}_1^\alpha$. This spin model can be converted to fermions by defining the $2N$ Majorana operators γ_k via

$$\gamma_{2k-1} = \sigma_z^{\otimes(k-1)} \otimes \sigma_x \otimes \mathbb{1}^{\otimes(N-k)}, \quad (\text{A3})$$

$$\gamma_{2k} = \sigma_z^{\otimes(k-1)} \otimes \sigma_y \otimes \mathbb{1}^{\otimes(N-k)}. \quad (\text{A4})$$

The Ising Hamiltonian then takes the form

$$\hat{H}_1 = \frac{i}{2} \left(\gamma_1 \gamma_{2N} P + J \sum_{k=1}^{N-1} \gamma_{2k} \gamma_{2k+1} + h \sum_{k=1}^N \gamma_{2k-1} \gamma_{2k} \right). \quad (\text{A5})$$

Here P is the total parity operator $\prod_k Z_k = \prod_k (-i \gamma_{2k-1} \gamma_{2k})$. At the critical point $J = h$, the Hamiltonian thus simplifies to

$$\hat{H} = \frac{i}{2} \left(\gamma_1 \gamma_{2N} P + \sum_{k=1}^{2N-1} \gamma_k \gamma_{k+1} \right), \quad (\text{A6})$$

which leads for $N \rightarrow \infty$ to the lattice model of the $c = \frac{1}{2}$ CFT. The critical Ising Hamiltonian as displayed in the main text (7) corresponds to $J = h = 1$.

Covariance matrix. For the critical ground state vector $|0\rangle$ which has a positive total parity, all correlations are encoded in the Majorana covariance matrix

$$\Omega_{j,k} = \frac{i}{2} \langle 0 | [\gamma_j, \gamma_k] | 0 \rangle, \quad (\text{A7})$$

which in the infinite system size limit takes the form

$$\Omega_{j,k} = \begin{cases} 0 & k = j \\ \frac{(-1)^{k-j}-1}{\pi(k-j)} & k \neq j \end{cases}. \quad (\text{A8})$$

Fermionic subsystem. We first consider the critical Ising model from the perspective of fermions, *i.e.*, locality is associated by the anti-commuting variables γ_i . A subsystem consisting of two sites ($w/\delta = 1$) separated by $d/w = d/\delta$ sites is then fully characterized by the restriction of the covariance matrix introduced in (A8) and explicitly given by

$$\Omega_{AB}^{\text{fer}} = \begin{pmatrix} & -\frac{2}{\pi} & & -\frac{2}{(2d/w+3)\pi} \\ \frac{2}{\pi} & & -\frac{2}{(2d/w+1)\pi} & \\ & \frac{2}{(2d/w+1)\pi} & \frac{2}{\pi} & -\frac{2}{\pi} \\ \frac{2}{(2d/w+3)\pi} & & & \end{pmatrix}, \quad (\text{A9})$$

from which we find $\Delta = \frac{1}{2}$. The associated fermionic density operator is then

$$\rho_{AB}^{\text{fer}} \sim \begin{pmatrix} D & & \frac{1}{2\pi} \epsilon_{\frac{1}{2}} \\ & E & \\ & & E \\ \frac{1}{2\pi} \epsilon_{\frac{1}{2}} & & & F \end{pmatrix} \quad (\text{A10})$$

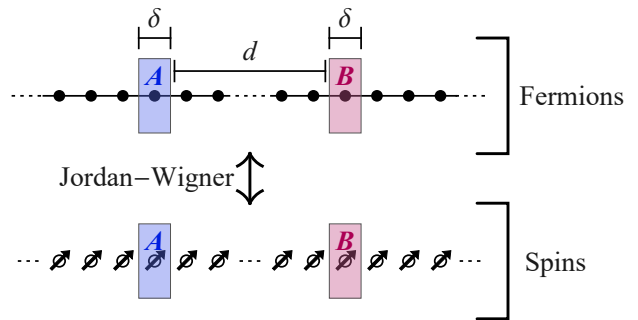


FIG. 3. Subsystem setup of our analytical limits for fermions (top) with an inherent ordering and spins (bottom) without one. In both systems, we consider the subsystem AB consisting of two single sites A and B separated by d/δ sites.

for $\epsilon_{\frac{1}{2}} = w/d$. If we further restrict to a single site, we find the following covariance matrix and density operator:

$$\Omega_A^f = \begin{pmatrix} \frac{2}{\pi} & -\frac{2}{\pi} \\ \frac{2}{\pi} & -\frac{2}{\pi} \end{pmatrix} \text{ with } \rho_A^f = \begin{pmatrix} \frac{1}{2} - \frac{1}{\pi} & \\ & \frac{1}{2} + \frac{1}{\pi} \end{pmatrix}. \quad (\text{A11})$$

Spin subsystem. We can perform a similar calculation in the original Ising spin system whose reduced density matrices can be constructed from the fermionic covariance matrix [55]. We need not repeat the single interval case, as entanglement entropies of connected regions are equivalent under a Jordan-Wigner transformation. However, we still need the reduced density matrix of a system of $1 + 1$ sites in the large d limit, which we find to be

$$\rho_{AB}^{\text{spin}} \sim \begin{pmatrix} D & & & C\epsilon_{\frac{1}{8}} \\ & E & C\epsilon_{\frac{1}{8}} & \\ & C\epsilon_{\frac{1}{8}} & E & \\ C\epsilon_{\frac{1}{8}} & & & F \end{pmatrix}. \quad (\text{A12})$$

Here, the constant C corresponds to the expectation value of an operator nonlocal in fermions, and can be computed from

$$C = \lim_{n \rightarrow \infty} \left(\frac{2}{\pi} \right)^n \frac{n^{1/4}}{4} \det M^n, \quad (\text{A13})$$

where M^n is defined as the $n \times n$ matrix

$$M_{j,k}^n = \begin{cases} \frac{(-1)^{k-j}}{2(k-j)+1} & j \leq k \\ \frac{(-1)^{j-k+1}}{2(j-k)-1} & j > k \end{cases}. \quad (\text{A14})$$

Using this construction, one finds [61]

$$C = \frac{e^{3\zeta'(-1)}}{2^{23/12}} \approx 0.1612506. \quad (\text{A15})$$

Mutual information and EoP for fermions. While we studied MI and EoP for spins in the main text, we

are now considering them for two sites separated by d in the fermionic picture. In this case, the state ρ_{AB}^f is Gaussian and fully characterized by the covariance matrix Ω_{AB}^f .

For the MI $I(A : B)$, we need to compute the von Neumann entropy of a single site $S_A = S_B$ and of both sites S_{AB} . Such a von Neumann can be computed from the eigenvalues of the covariance matrix Ω associated to the respective Gaussian state ρ . As an antisymmetric matrix, Ω_{AB}^f has pairs of purely imaginary eigenvalues $\pm i\lambda_k$, from which one can compute the von Neumann entropies as $S(\rho) = -\sum_{\pm, i} \frac{1 \pm \lambda_i}{2} \log \frac{1 \pm \lambda_i}{2}$ leading to

$$S_A = -\frac{\pi+2}{2\pi} \log \frac{\pi+2}{2\pi} - \frac{\pi-2}{2\pi} \log \frac{\pi-2}{2\pi} \approx 0.474 \quad (\text{A16})$$

$$S_{AB} = \sum_{k=1}^n \left(-\frac{1+\lambda_k}{2} \log \frac{1+\lambda_k}{2} - \frac{1-\lambda_k}{2} \log \frac{1-\lambda_k}{2} \right), \quad (\text{A17})$$

where the eigenvalues of Ω_{AB}^f are to leading order

$$\lambda_{1,2} = \frac{1}{\pi} \left(2 \pm \frac{3}{4} \epsilon_{\frac{1}{2}}^2 \right) + \mathcal{O}(\epsilon_{\frac{1}{2}}^2). \quad (\text{A18})$$

We can similarly expand $S_{1+1} \equiv S_{AB}$ at large d , which results in the MI

$$I^{\text{fer}}(A : B) = 2S_A - S_{AB} \sim \frac{\log \frac{\pi+2}{\pi-2}}{4\pi} \epsilon_{\frac{1}{2}}^2 + \mathcal{O}(\epsilon_{\frac{1}{2}}^2). \quad (\text{A19})$$

This reproduces the correct continuum power law of fermionic MI, but yields a coefficient lower than the continuum value (5) which also matches the large-distance expansion of earlier results for Dirac fermions [62]

$$I(A : B) = \frac{c}{3} \log \frac{(d+w)^2}{d(2w+d)} = \frac{1}{6} \epsilon_{\frac{1}{2}}^2 + \mathcal{O}(\epsilon_{\frac{1}{2}}^2). \quad (\text{A20})$$

We can follow a similar strategy to compute the EoP in the fermionic subsystem of two sites separated by d/δ sites. We purify Ω_{AB} in the limit $d/\delta \rightarrow \infty$ as

$$\Omega^{(0)} = \left(\begin{array}{cc|cc} -G & & L & \\ G & & L & \\ & -G & & L \\ \hline & G & & L \\ -L & & -G & \\ & -L & G & \\ & & & -G \\ & -L & & G \end{array} \right) \quad (\text{A21})$$

associated to $A + B + A' + B'$ with $G = \frac{2}{\pi}$ and $L = \sqrt{1-G^2}$, whose EE $S_{AA'}$ is zero and we thus have $\lim_{d \rightarrow \infty} E_P = 0$, *i.e.*, the EoP vanishes for large d/δ , as expected.

In order to find the asymptotic behaviour of E_P , we need to study the variation of the eigenvalues λ of $\Omega_{AA'}$ when perturbing Ω according to

$$\Omega \sim \Omega^{(0)} + \epsilon_{\frac{1}{2}} \Omega^{(1)} + \frac{1}{2} \epsilon_{\frac{1}{2}}^2 \Omega^{(2)} \quad \text{as } \epsilon_{\frac{1}{2}} \rightarrow 0. \quad (\text{A22})$$

The requirement of Ω representing a purification implies $\Omega^2 = -\mathbb{1}$, which induces the constraints

$$\begin{aligned} \Omega^{(0)}\Omega^{(1)} + \Omega^{(1)}\Omega^{(0)} &= 0, \\ 2(\Omega^{(1)})^2 + \Omega^{(0)}\Omega^{(2)} + \Omega^{(2)}\Omega^{(0)} &= 0. \end{aligned} \quad (\text{A23})$$

We further require that the restrictions $\Omega_{AB}^{(1)}$ and $\Omega_{AB}^{(2)}$ matches the ones of (A9) expanded in $\epsilon_{\frac{1}{2}}$, *i.e.*,

$$\Omega_{AB}^{(1)} = \begin{pmatrix} & & -\frac{1}{\pi} \\ & -\frac{1}{\pi} & \\ \frac{1}{\pi} & & \end{pmatrix}, \quad \Omega_{AB}^{(2)} = \begin{pmatrix} & & \frac{3}{\pi} \\ & -\frac{1}{\pi} & \\ -\frac{3}{\pi} & & \end{pmatrix}, \quad (\text{A24})$$

The equations (A23) and (A24) can be solved iteratively up to some free variables. We first solve $\Omega^{(1)}$ in terms of $\Omega^{(0)}$ and then $\Omega^{(2)}$ in terms of $\Omega^{(0)}$ and $\Omega^{(1)}$.

In order to find asymptotics of the symplectic eigenvalues λ_i , we can use the fact that $\text{Tr}(\Omega_{AA'}^2) = -2(\lambda_1^2 + \lambda_2^2)$ and $\text{Tr}(\Omega_{AA'}^4) = 2\lambda_1^4 + \lambda_2^4$ to solve for the asymptotics of λ_i to be given by

$$\lambda_1 = \lambda_2 \sim 1 - \alpha \epsilon_{\frac{1}{2}}^2 \quad \text{as } \epsilon_{\frac{1}{2}} \rightarrow 0, \quad (\text{A25})$$

where α will depend on some of the free parameters contained in $\Omega^{(1)}$ and $\Omega^{(2)}$. With this trick, one finds

$$\begin{aligned} \alpha &= \frac{x_{14}a_{23} - x_{13}x_{24} + \pi^{-2}}{2} + \frac{G(x_{14} - x_{23})\pi^{-1}}{2L} \\ &+ \frac{(x_{14} - x_{23})^2 + (x_{13} + x_{24})^2}{4L^2}, \end{aligned} \quad (\text{A26})$$

where the variables x_{ij} represent unconstrained entries in the block $\Omega_{AB, A'B'}^{(1)}$. In order to find the asymptotics of EoP, we need to minimize α over these parameters to find the smallest possible EE $S_{AA'}$. This minimum can be computed analytically to be

$$\alpha = \frac{1}{8 + 2\pi^2} \approx 0.03605. \quad (\text{A27})$$

Expanding $S_{AA'} \sim \sum_i (\log 2 - \frac{\lambda_i}{2})$ through λ up to second order in d gives the asymptotics

$$\begin{aligned} E_P &= \epsilon_{\frac{1}{2}}^2 \left(\alpha \log(\epsilon_{\frac{1}{2}}^{-2}) + \alpha \log \frac{2e}{\alpha} \right) \\ &\approx \epsilon_{\frac{1}{2}}^2 \left(0.036 \log(\epsilon_{\frac{1}{2}}^{-2}) + 0.18 \right), \end{aligned} \quad (\text{A28})$$

which agrees with the form (19). Note that the simplicity of Gaussian states allowed us to even find the analytical form of the constant offset. The accuracy of this analytical prediction was tested numerically, for which we presented the results in figure 2 in the main text.

Numerical approach and asymmetric purifications. Our numerical methods are based on [29, 57, 63],

		$N_{A'} + N_{B'}$						
		1 + 1	1 + 2	2 + 1	1 + 3	2 + 2	3 + 1	
$N_A + N_B$	1 + 1	$d = \delta$	0.382	0.382	0.382	0.382	0.382	0.382
		$d = 2\delta$	0.333	0.333	0.333	0.333	0.333	0.333
		$d = 3\delta$	0.306	0.306	0.306	0.306	0.306	0.306
		$d = 2\delta$	0.292	0.292	0.292	0.292	0.292	0.292
	1 + 2	$d = \delta$	n.a.	0.412	0.438	0.412	0.412	0.440
		$d = 2\delta$		0.368	0.412	0.368	0.368	0.415
		$d = 3\delta$		0.345	0.394	0.345	0.345	0.398
		$d = 4\delta$		0.335	0.385	0.335	0.335	0.389

TABLE I. Numerical evidence for optimality of certain minimal purifications. The table shows the values of the optimization for different choices of the system dimensions and of d . The true EoP values (the minimum optimization values) are highlighted in yellow, with the darker shade indicating the lowest-dimensional purification for which the EoP is obtained.

which outline the construction of an efficient algorithm for local optimization over Gaussian states, based on a gradient descent approach exploiting the natural Lie group parametrization of the state manifolds. Our numerical results are obtained using an adaptation of this algorithm to the non-Gaussian case of interest.

To compute the EoP as given in (4), we minimise the entanglement entropy S over the manifold \mathcal{M} of purified state density matrices. We first purify our initial mixed density matrix to a 2^N -dimensional pure ρ_1 via the Schmidt decomposition. Here, $N = \sum_X N_X$ with N_X denoting the physical degrees of freedom in subsystem X . We parametrize elements $\rho_U \in \mathcal{M}$ by transformations $U = \mathbb{1} \otimes \tilde{U}$ with $\tilde{U} \in \text{U}(2^{N_{A'}+N_{B'}})$, so that $\rho_U = U\rho_1 U^{-1}$. The tensor product signifies that U only acts non-trivially on degrees of freedom in A' and B' . We then optimize by performing iterative steps along directions in \mathcal{M} which locally minimize $S_{AA'}$ [29, 57],

$$U_{n+1} = U_n e^{tK_n}. \quad (\text{A29})$$

Here, $K_n = \sum_\mu \mathcal{F}^\mu(U_n) \Xi_\mu / \|\mathcal{F}\|^2$ and $\mathcal{F}^\mu : \mathcal{M} \rightarrow \mathbb{R}$ is the gradient descent vector field

$$\mathcal{F}^\mu(U) = -\frac{\partial}{\partial s} S(U e^{s\Xi_\mu} \rho_1 e^{-s\Xi_\mu} U^{-1})|_{s=0} \quad (\text{A30})$$

with $\{\Xi_\mu\}$ as basis of $\mathfrak{u}(2^{N_{A'}+N_{B'}})$. We choose $U_0 = \mathbb{1}$ and we pick $0 < t < 1$ in such a way that the value of $S_{AA'}$ decreases with successive steps.

The $\{\Xi_\mu\}$ span the tangent space at $U = \mathbb{1}$ and, due to the left-invariance of the Riemannian metric on \mathcal{M} , form orthonormal bases for the tangent spaces at all other points in \mathcal{M} , too, where Ξ_μ is identified with the tangent vector to the curve $\gamma(s) = U e^{s\Xi_\mu}$ at $\gamma(0)$ [57]. This saves us having to re-evaluate the matrix representation of the metric at each step, as we would have to if we had chosen a coordinate parametrisation of \mathcal{M} . While this

makes our algorithm more efficient than a naive gradient descent, the numerically accessible range is still highly limited: since $N_{A'} + N_{B'} \geq N_A + N_B$, the dimension of \mathcal{M} is at least $\dim_{\mathbb{C}}(2^{N_{A'}+N_{B'}}) = 2^{2N_{A'}+2N_{B'}} - 1$ and (A29) requires exponentiation of at least $2^{(N_A+N_B)} \times 2^{(N_A+N_B)}$ matrices, with a typical step count of several hundred. This becomes extremely slow on a powerful Desktop computer for $N_{A'} + N_{B'} \geq 5$. For the symmetric purifications in the main text this corresponds with $w > 2\delta$, which explains the regime we were able to explore.

Given this limitation on our numerical capabilities, it is instructive to ask whether an optimization over minimal purifications corresponding with $N_{A'} + N_{B'} = N_A + N_B$ yields the true minimum of EE – not least because for large systems this becomes the only numerically viable choice. A natural follow-up question is whether among the choices of minimal purifications, the intuitive choice of $N_{A'} = N_A$ and $N_{B'} = N_B$ suffices to reach the true minimum defined as EoP. More pertinently, we might ask whether it is even possible to reach the true minimum with a minimal purification for which $N_{A'} \neq N_A$ and $N_{B'} \neq N_B$. In [57], a combination of numerical and analytical evidence was provided to show that the answer to this question is in affirmative for Gaussian states. While limited by the greater numerical challenge in the non-Gaussian case, we present similar numerical evidence in Table I to show that the same may be said for our model: the true minimum can only be reached if $N_{A'} \geq N_A$ and $N_{B'} \geq N_B$, which indicates that the lowest-dimensional purification for which the EoP can be obtained is the minimal purification with $N_{A'} = N_A$ and $N_{B'} = N_B$.

* hugo.camargo@aei.mpg.de

† lucas.hackl@unimelb.edu.au

‡ michal.p.heller@aei.mpg.de; *On leave of absence from:* National Centre for Nuclear Research, Pasteura 7, 02-093 Warsaw, Poland

§ a.jahn@fu-berlin.de

¶ benet.windt17@imperial.ac.uk

- [1] Juan Martin Maldacena, “The Large N limit of superconformal field theories and supergravity,” *Int. J. Theor. Phys.* **38**, 1113–1133 (1999), arXiv:hep-th/9711200.
- [2] S.S. Gubser, Igor R. Klebanov, and Alexander M. Polyakov, “Gauge theory correlators from noncritical string theory,” *Phys. Lett. B* **428**, 105–114 (1998), arXiv:hep-th/9802109.
- [3] Edward Witten, “Anti-de Sitter space and holography,” *Adv. Theor. Math. Phys.* **2**, 253–291 (1998), arXiv:hep-th/9802150.
- [4] H. Casini and M. Huerta, “Entanglement entropy in free quantum field theory,” *J. Phys. A* **42**, 504007 (2009), arXiv:0905.2562 [hep-th].
- [5] Daniel Harlow, “Jerusalem Lectures on Black Holes and Quantum Information,” *Rev. Mod. Phys.* **88**, 015002 (2016), arXiv:1409.1231 [hep-th].

- [6] Mukund Rangamani and Tadashi Takayanagi, *Holographic Entanglement Entropy*, Vol. 931 (Springer, 2017) arXiv:1609.01287 [hep-th].
- [7] Leonard Susskind, “Three Lectures on Complexity and Black Holes,” (2018) arXiv:1810.11563 [hep-th].
- [8] Matthew Headrick, “Lectures on entanglement entropy in field theory and holography,” (2019), arXiv:1907.08126 [hep-th].
- [9] Rafael D Sorkin, “On the entropy of the vacuum outside a horizon,” in *Tenth International Conference on General Relativity and Gravitation (held in Padova, 4-9 July, 1983), Contributed Papers*, Vol. 2 (1983) pp. 734–736, arXiv:1402.3589.
- [10] Ingo Peschel, “Calculation of reduced density matrices from correlation functions,” *Journal of Physics A: Mathematical and General* **36**, L205 (2003).
- [11] Christian Weedbrook, Stefano Pirandola, Raúl García-Patrón, Nicolas J. Cerf, Timothy C. Ralph, Jeffrey H. Shapiro, and Seth Lloyd, “Gaussian quantum information,” *Reviews of Modern Physics* **84**, 621–669 (2012).
- [12] Eugenio Bianchi, Lucas Hackl, and Nelson Yokomizo, “Entanglement entropy of squeezed vacua on a lattice,” *Phys. Rev. D* **92**, 085045 (2015), arXiv:1507.01567 [hep-th].
- [13] Lucas Hackl and Eugenio Bianchi, “Bosonic and fermionic Gaussian states from Kähler structures,” (2020), arXiv:2010.15518 [quant-ph].
- [14] Christoph Holzhey, Finn Larsen, and Frank Wilczek, “Geometric and renormalized entropy in conformal field theory,” *Nucl. Phys. B* **424**, 443–467 (1994), arXiv:hep-th/9403108.
- [15] Pasquale Calabrese and John L. Cardy, “Entanglement entropy and quantum field theory,” *J. Stat. Mech.* **0406**, P06002 (2004), arXiv:hep-th/0405152 [hep-th].
- [16] Pasquale Calabrese and John Cardy, “Entanglement entropy and conformal field theory,” *J. Phys. A* **42**, 504005 (2009), arXiv:0905.4013 [cond-mat.stat-mech].
- [17] Pasquale Calabrese, John Cardy, and Erik Tonni, “Entanglement entropy of two disjoint intervals in conformal field theory,” *J. Stat. Mech.* **0911**, P11001 (2009), arXiv:0905.2069 [hep-th].
- [18] John Cardy, “Some results on the mutual information of disjoint regions in higher dimensions,” *J. Phys.* **A46**, 285402 (2013), arXiv:1304.7985 [hep-th].
- [19] Tomonori Ugajin, “Mutual information of excited states and relative entropy of two disjoint subsystems in CFT,” *JHEP* **10**, 184 (2017), arXiv:1611.03163 [hep-th].
- [20] M. B. Hastings, “An area law for one-dimensional quantum systems,” *J. Stat. Mech.* **0708**, P08024 (2007), arXiv:0705.2024 [quant-ph].
- [21] G. Vidal, “Class of Quantum Many-Body States That Can Be Efficiently Simulated,” *Phys. Rev. Lett.* **101**, 110501 (2008), arXiv:quant-ph/0610099.
- [22] Shinsei Ryu and Tadashi Takayanagi, “Holographic derivation of entanglement entropy from AdS/CFT,” *Phys. Rev. Lett.* **96**, 181602 (2006), arXiv:hep-th/0603001.
- [23] Veronika E. Hubeny, Mukund Rangamani, and Tadashi Takayanagi, “A Covariant holographic entanglement entropy proposal,” *JHEP* **07**, 062 (2007), arXiv:0705.0016 [hep-th].
- [24] Aitor Lewkowycz and Juan Maldacena, “Generalized gravitational entropy,” *JHEP* **08**, 090 (2013), arXiv:1304.4926 [hep-th].
- [25] Xi Dong, Aitor Lewkowycz, and Mukund Rangamani, “Deriving covariant holographic entanglement,” *JHEP* **11**, 028 (2016), arXiv:1607.07506 [hep-th].
- [26] Barbara M. Terhal, Michał Horodecki, Debbie W. Leung, and David P. DiVincenzo, “The entanglement of purification,” *Journal of Mathematical Physics* **43**, 4286–4298 (2002).
- [27] Arpan Bhattacharyya, Tadashi Takayanagi, and Koji Umemoto, “Entanglement of Purification in Free Scalar Field Theories,” *JHEP* **04**, 132 (2018), arXiv:1802.09545 [hep-th].
- [28] Arpan Bhattacharyya, Alexander Jahn, Tadashi Takayanagi, and Koji Umemoto, “Entanglement of Purification in Many Body Systems and Symmetry Breaking,” *Phys. Rev. Lett.* **122**, 201601 (2019), arXiv:1902.02369 [hep-th].
- [29] Hugo A. Camargo, Lucas Hackl, Michal P. Heller, Alexander Jahn, Tadashi Takayanagi, and Bennet Windt, “Entanglement and Complexity of Purification in (1+1)-dimensional free Conformal Field Theories,” (2020), arXiv:2009.11881 [hep-th].
- [30] Hayato Hirai, Kotaro Tamaoka, and Tsuyoshi Yokoya, “Towards Entanglement of Purification for Conformal Field Theories,” *PTEP* **2018**, 063B03 (2018), arXiv:1803.10539 [hep-th].
- [31] Pawel Caputa, Masamichi Miyaji, Tadashi Takayanagi, and Koji Umemoto, “Holographic Entanglement of Purification from Conformal Field Theories,” *Phys. Rev. Lett.* **122**, 111601 (2019), arXiv:1812.05268 [hep-th].
- [32] Wu-Zhong Guo, “Entanglement of purification and disentanglement in CFTs,” *JHEP* **09**, 080 (2019), arXiv:1904.12124 [hep-th].
- [33] Tadashi Takayanagi and Koji Umemoto, “Entanglement of purification through holographic duality,” *Nature Phys.* **14**, 573–577 (2018), arXiv:1708.09393 [hep-th].
- [34] Phuc Nguyen, Trithep Devakul, Matthew G. Halbasch, Michael P. Zaletel, and Brian Swingle, “Entanglement of purification: from spin chains to holography,” *JHEP* **01**, 098 (2018), arXiv:1709.07424 [hep-th].
- [35] Bartłomiej Czech, Joanna L. Karczmarek, Fernando Nogueira, and Mark Van Raamsdonk, “The Gravity Dual of a Density Matrix,” *Class. Quant. Grav.* **29**, 155009 (2012), arXiv:1204.1330 [hep-th].
- [36] Aron C. Wall, “Maximin Surfaces, and the Strong Subadditivity of the Covariant Holographic Entanglement Entropy,” *Class. Quant. Grav.* **31**, 225007 (2014), arXiv:1211.3494 [hep-th].
- [37] Matthew Headrick, Veronika E. Hubeny, Albion Lawrence, and Mukund Rangamani, “Causality & holographic entanglement entropy,” *JHEP* **12**, 162 (2014), arXiv:1408.6300 [hep-th].
- [38] Ning Bao and Illan F. Halpern, “Holographic Inequalities and Entanglement of Purification,” *JHEP* **03**, 006 (2018), arXiv:1710.07643 [hep-th].
- [39] Koji Umemoto and Yang Zhou, “Entanglement of Purification for Multipartite States and its Holographic Dual,” *JHEP* **10**, 152 (2018), arXiv:1805.02625 [hep-th].
- [40] Kotaro Tamaoka, “Entanglement Wedge Cross Section from the Dual Density Matrix,” *Phys. Rev. Lett.* **122**, 141601 (2019), arXiv:1809.09109 [hep-th].
- [41] Ning Bao and Illan F. Halpern, “Conditional and Multipartite Entanglements of Purification and Holography,” *Phys. Rev. D* **99**, 046010 (2019), arXiv:1805.00476 [hep-th].

- th].
- [42] Ricardo Espíndola, Alberto Guijosa, and Juan F. Pedraza, “Entanglement Wedge Reconstruction and Entanglement of Purification,” *Eur. Phys. J. C* **78**, 646 (2018), arXiv:1804.05855 [hep-th].
- [43] Run-Qiu Yang, Cheng-Yong Zhang, and Wen-Ming Li, “Holographic entanglement of purification for thermofield double states and thermal quench,” *JHEP* **01**, 114 (2019), arXiv:1810.00420 [hep-th].
- [44] Yasunori Nomura, Pratik Rath, and Nico Salzetta, “Pulling the Boundary into the Bulk,” *Phys. Rev. D* **98**, 026010 (2018), arXiv:1805.00523 [hep-th].
- [45] Peng Liu, Yi Ling, Chao Niu, and Jian-Pin Wu, “Entanglement of Purification in Holographic Systems,” *JHEP* **09**, 071 (2019), arXiv:1902.02243 [hep-th].
- [46] Jonathan Harper and Matthew Headrick, “Bit threads and holographic entanglement of purification,” *JHEP* **08**, 101 (2019), arXiv:1906.05970 [hep-th].
- [47] Komeil Babaei Velni, M. Reza Mohammadi Mozaffar, and M. H. Vahidinia, “Some Aspects of Entanglement Wedge Cross-Section,” *JHEP* **05**, 200 (2019), arXiv:1903.08490 [hep-th].
- [48] B. Amrahi, M. Ali-Akbari, and M. Asadi, “Holographic entanglement of purification near a critical point,” *Eur. Phys. J. C* **80**, 1152 (2020), arXiv:2004.02856 [hep-th].
- [49] Parul Jain and Subhash Mahapatra, “Mixed state entanglement measures as probe for confinement,” *Phys. Rev. D* **102**, 126022 (2020), arXiv:2010.07702 [hep-th].
- [50] Xi Dong, Daniel Harlow, and Aron C. Wall, “Reconstruction of Bulk Operators within the Entanglement Wedge in Gauge-Gravity Duality,” *Phys. Rev. Lett.* **117**, 021601 (2016), arXiv:1601.05416 [hep-th].
- [51] Pasquale Calabrese, John Cardy, and Erik Tonni, “Entanglement entropy of two disjoint intervals in conformal field theory II,” *J. Stat. Mech.* **1101**, P01021 (2011), arXiv:1011.5482 [hep-th].
- [52] Cesar Agón and Thomas Faulkner, “Quantum Corrections to Holographic Mutual Information,” *JHEP* **08**, 118 (2016), arXiv:1511.07462 [hep-th].
- [53] F. Iglói and I. Peschel, “On reduced density matrices for disjoint subsystems,” *EPL (Europhysics Letters)* **89**, 40001 (2010).
- [54] Maurizio Fagotti and Pasquale Calabrese, “Entanglement entropy of two disjoint blocks in XY chains,” *J. Stat. Mech.* **1004**, P04016 (2010), arXiv:1003.1110 [cond-mat.stat-mech].
- [55] Andrea Coser, Erik Tonni, and Pasquale Calabrese, “Partial transpose of two disjoint blocks in XY spin chains,” *J. Stat. Mech.* **1508**, P08005 (2015), arXiv:1503.09114 [cond-mat.stat-mech].
- [56] Andrea Coser, Erik Tonni, and Pasquale Calabrese, “Spin structures and entanglement of two disjoint intervals in conformal field theories,” *Journal of Statistical Mechanics: Theory and Experiment* **2016**, 053109 (2016).
- [57] Bennet Windt, Alexander Jahn, Jens Eisert, and Lucas Hackl, “Local optimization on pure Gaussian state manifolds,” (2020), arXiv:2009.11884 [quant-ph].
- [58] Lucas Hackl, Tommaso Guaita, Tao Shi, Jutho Haegeman, Eugene Demler, and Ignacio Cirac, “Geometry of variational methods: dynamics of closed quantum systems,” *SciPost Phys.* **9**, 048 (2020), arXiv:2004.01015 [quant-ph].
- [59] P. Di Francesco, P. Mathieu, and D. Senechal, *Conformal Field Theory*, Graduate Texts in Contemporary Physics (Springer-Verlag, New York, 1997).
- [60] Szilárd Szalay, Zoltán Zimborás, Mihály Máté, Gergely Barcza, Christian Schilling, and Örs Legeza, “Fermionic systems for quantum information people,” (2020), arXiv:2006.03087 [quant-ph].
- [61] B. McCoy, “Ising model: exact results,” *Scholarpedia* **5**, 10313 (2010), revision #137428.
- [62] H. Casini, C. D. Fosco, and M. Huerta, “Entanglement and alpha entropies for a massive Dirac field in two dimensions,” *J. Stat. Mech.* **0507**, P07007 (2005), arXiv:cond-mat/0505563 [cond-mat].
- [63] Lucas Hackl, Tommaso Guaita, Tao Shi, Jutho Haegeman, Eugene Demler, and Ignacio Cirac, “Geometry of variational methods: dynamics of closed quantum systems,” arXiv preprint arXiv:2004.01015 (2020).